

Supporting Materials for

Formation and Decomplexation Kinetics of Copper(II) Complexes with Cyclen Derivatives Having Mixed Carboxylate and Phosphonate Pendant Arms

R. Ševčík,^a J. Vaněk,^{a,b} R. Michaliová,^a P. Lubal,^{a,b}* P. Hermann,^c I. C. Santos^d, I. Santos^d, M. P. C. Campello,^d*

^a Department of Chemistry, Faculty of Science, Masaryk University, Kotlářská 2, 611 37 Brno, Czech Republic. E-mail: lubal@chemi.muni.cz, Fax: +420-54949 2494, Tel: +420-54949 5637.

^b Central European Institute of Technology (CEITEC), Masaryk University, Kamenice 5, 625 00 Brno, Czech Republic.

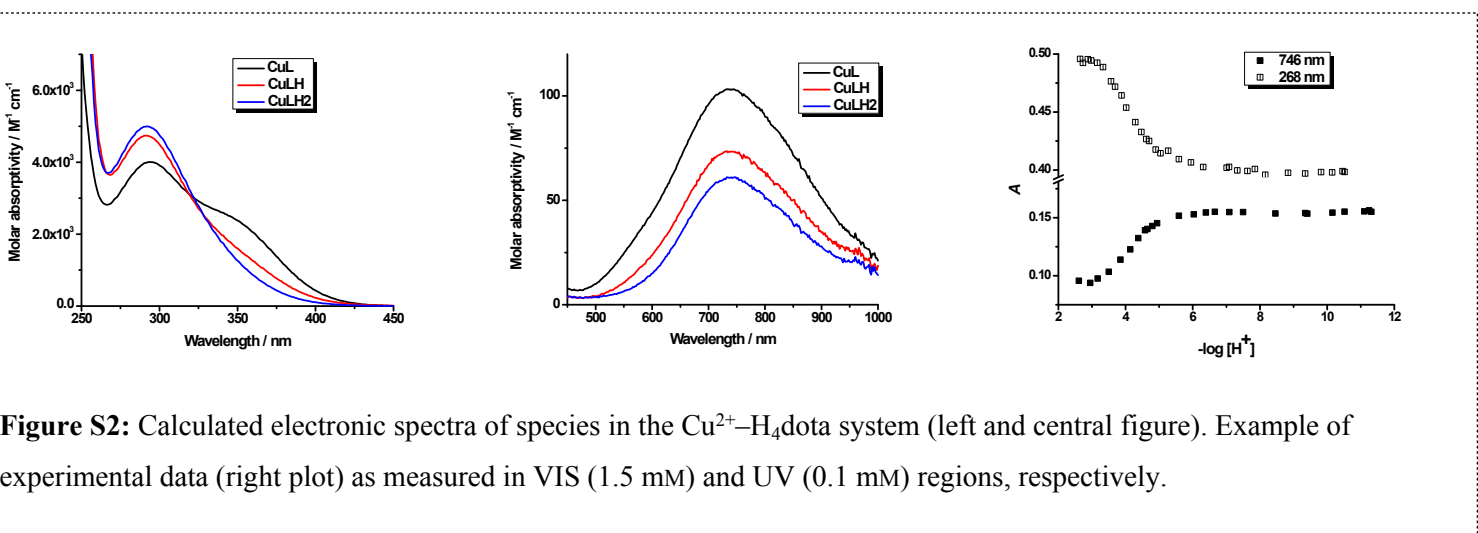
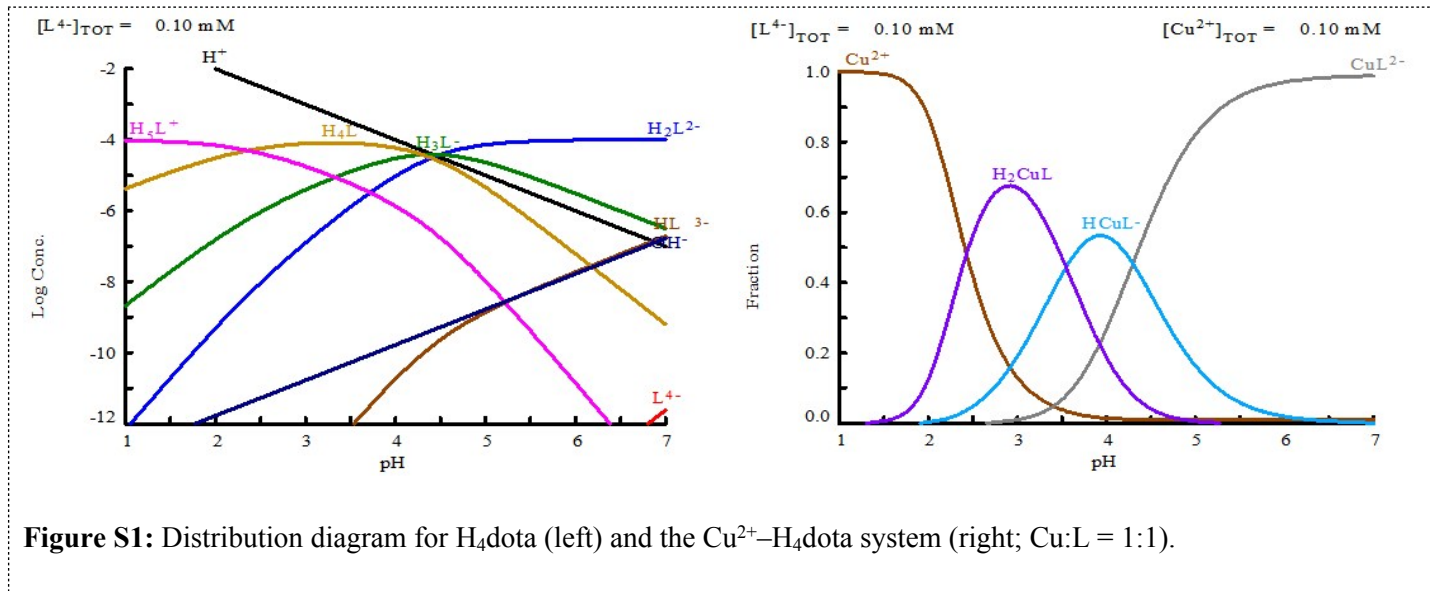
^c Department of Inorganic Chemistry, Faculty of Science, Universita Karlova (Charles University), Hlavova 2030, 128 40 Prague 2, Czech Republic.

^d Centro de Ciências e Tecnologias Nucleares, Instituto Superior Técnico, Universidade de Lisboa, Estrada Nacional 10, 2695-066 BobadelaLRS, Portugal. E-mail: pcampelo@ctn.tecnico.ulisboa.pt, Fax: +351-21-9946185, Tel: +351-21-9946233.

Content

Page

Figures S1+S3+S5+S7: Distribution diagram for Cu(II)-H ₄ dota + <i>trans</i> -H ₆ do2a2p + H ₄ dotp (Cu:L ratio 1:1) + H ₄ dotp (Cu:L ratio 2:1) systems, respectively	2–5
Figures S2+S4+S6+S8: Calculated electronic spectra of species in the Cu ²⁺ -H ₄ dota + <i>trans</i> -H ₆ do2a2p + H ₄ dotp (mononuclear complexes) + H ₄ dotp (dinuclear complexes) systems, respectively	2–5
Table S1: UV-Vis spectral parameters calculated for species present in Cu(II)-H ₄ dota-like ligand systems	6
Table S2: Summary of stepwise protonation constants of the title ligands	7
Table S3: Summary of derived equilibrium constants for systems with Cu(II) ion and the title ligands	7
Table S4: Overall protonation constants of H ₈ dotp ligand and stability constants for the Cu(II)-H ₈ dotp system	8
Table S5: Full set of derived equilibrium constants for the Cu(II)-H ₈ dotp system	8
Figure S9: Correlation of values of stability constant for copper(II) mononuclear and dinuclear complexes with basicity of macrocyclic ring	9
Figure S10: Correlation of values of stability constant for Cu(II) dinuclear complexes with basicity of pendant arms in the copper(II) mononuclear complex	9
Potentiometry of the Cu(II)-H₈dotp system – Experimental details	10
Figure S11: Distribution diagrams of the Cu(II)-H ₈ dotp system for L:Cu 1:1 and 2:1 molar ratios	11
Figure S12+S13: Dependence of the second-order formation rate constants, <i>k</i> _f , for the Cu(II) complexes with H ₄ dota, <i>trans</i> -H ₆ do2a2p and H ₈ dotp, H ₇ doa3p on pH, respectively	12
Figure S14+S16+S18: Example of time change of absorption spectra in the course of formation of the [Cu(dotp)] ⁶⁻ , [Cu(doa3p)] ⁵⁻ and [Cu(<i>trans</i> -do2a2p)] ⁴⁻ complex, respectively	13–15
Figure S15+S17+S19: Dependence of pseudo-first order rate constant on Cu(II) ion concentration for formation of the [Cu(dotp)] ⁶⁻ , [Cu(doa3p)] ⁵⁻ and [Cu(<i>trans</i> -do2a2p)] ⁴⁻ complexes, respectively	13–15
Figure S20: LFER plot showing correlation of partial rate constants of formation of Cu(II) complexes for triple charged species and double charged species	16
Figure S21: Dependence of rate constants for reaction of triple-charged species of the ligands with Cu(II) on a number of phosphonic acid groups	16
Figure S22: LFER plot showing correlation of partial rate constants (for triply negative species) for formation of copper(II) complexes	16
Figure S23+S25+S27: Time change in the absorption spectra in the course of decomplexation of the [Cu(dotp)] ⁶⁻ , [Cu(doa3p)] ⁵⁻ and [Cu(<i>trans</i> -do2a2p)] ⁴⁻ complexes, respectively	17–19
Figure S24+S26: Pseudo-first order rate constants as function of proton concentration for acid-assisted decomplexation of the [Cu(dotp)] ⁶⁻ and [Cu(doa3p)] ⁵⁻ complexes, respectively	17–18
Table S5. Kinetic parameters for acid-assisted decomplexation of Cu(II) complexes of the studied ligands	20
Figure S28: Dependence of rate constants for acid-assisted dissociation of Cu(II) complexes on the number of phosphonic acid groups in H ₄ dota and its analogues	21
Figure S29: Dependence of rate constants for acid-assisted dissociation of the Cu(II) complexes on basicity of the ligands	21
Figure S30: Correlation of rate constants for acid-assisted dissociation of Cu(II) complexes with basicity of pendant arms of the Cu(II) complexes	22
Figure S31: Isokinetic plot for Cu(II) complex dissociation	23
Table S6: Experimental data for determination of crystal structure of KH ₆ doa3p·3H ₂ O	24
Table S7 Selected bond length and angles of the KH ₆ doa3p·3H ₂ O in the solid-state	25
Figure S32: Crystal packing of KH ₆ doa3p·3H ₂ O in solid state	26
References	27



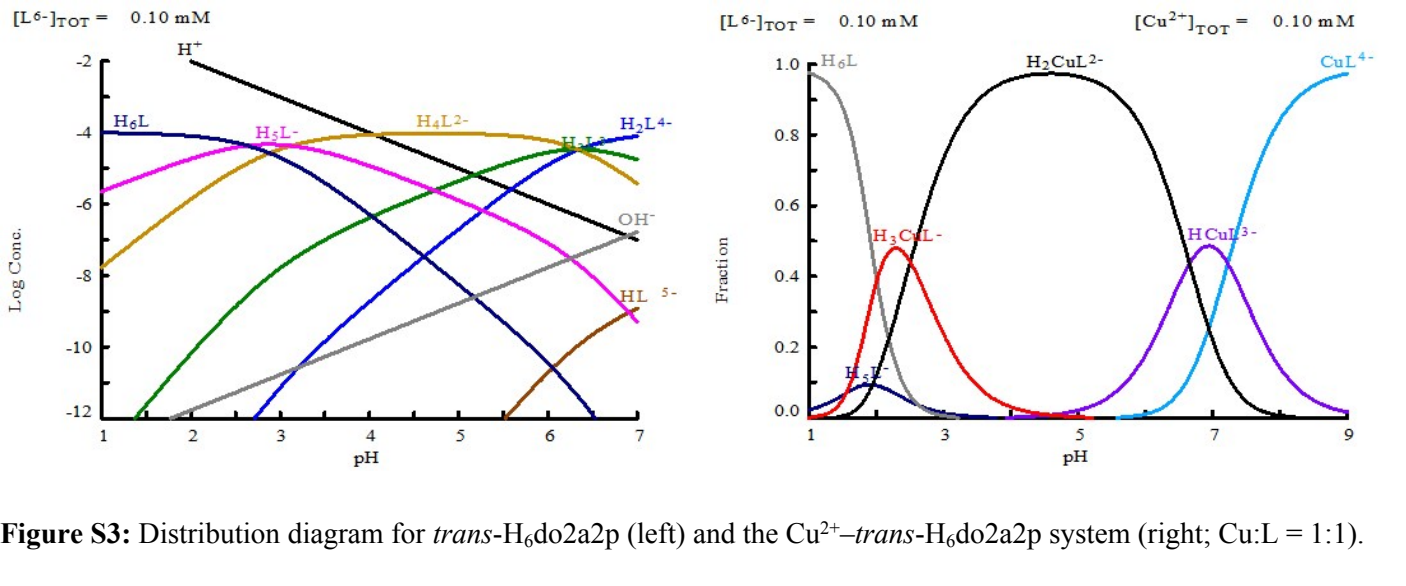


Figure S3: Distribution diagram for *trans*-H₆do2a2p (left) and the Cu²⁺-*trans*-H₆do2a2p system (right; Cu:L = 1:1).

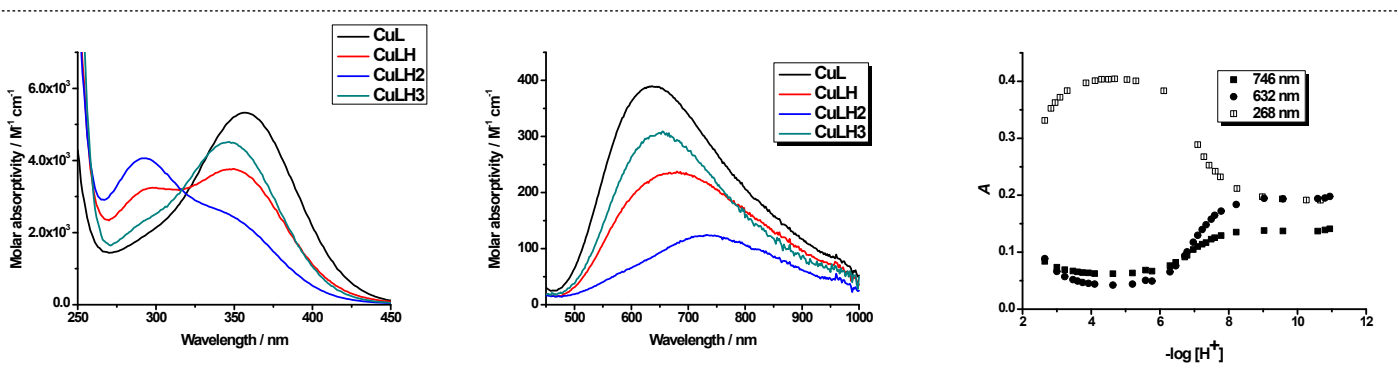


Figure S4: Calculated electronic spectra of species in the Cu²⁺-*trans*-H₆do2a2p system (left and central figure). Example of experimental data (right plot) as measured in VIS (0.5 mM) and UV (0.1 mM) regions, respectively.

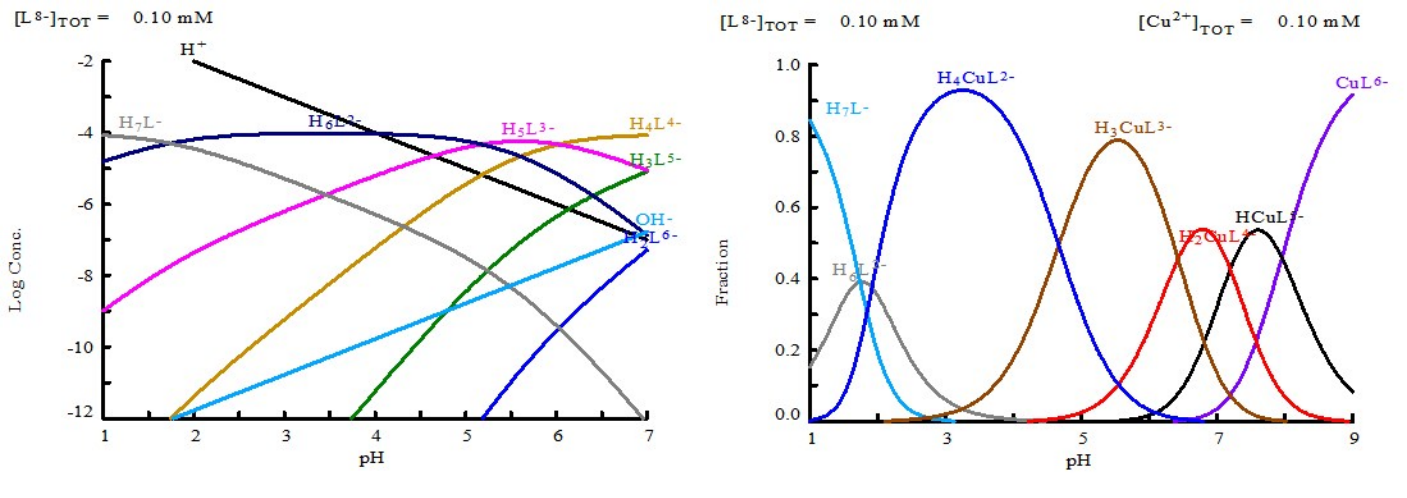


Figure S5: Distribution diagram for H_8dotp (left) and the $\text{Cu}^{2+}-\text{H}_8\text{dotp}$ system (right; $\text{Cu}: \text{L} = 1:1$).

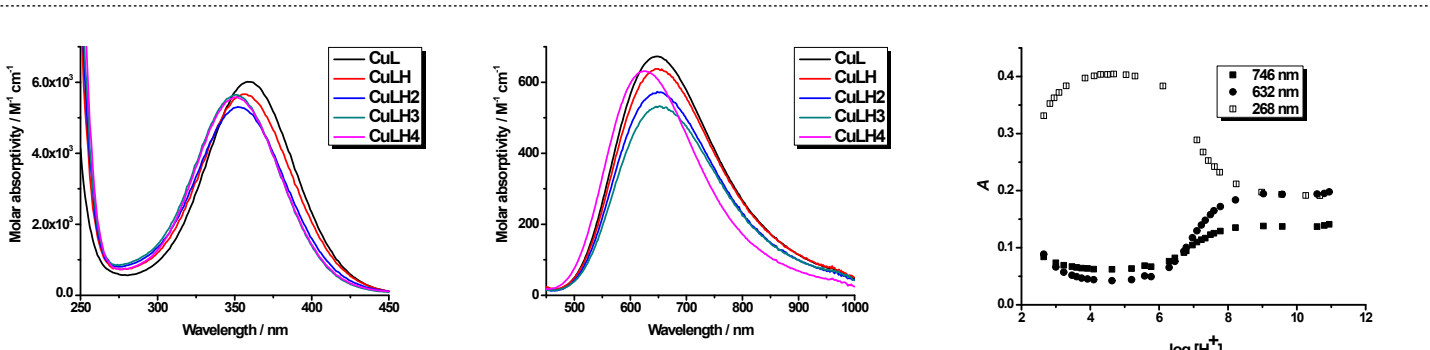


Figure S6: Calculated electronic spectra of mononuclear species in the $\text{Cu}^{2+}-\text{H}_8\text{dotp}$ system (left and central figures). Example of experimental data (right) as measured in VIS (1.0 mM) and UV (0.1 mM) regions, respectively.

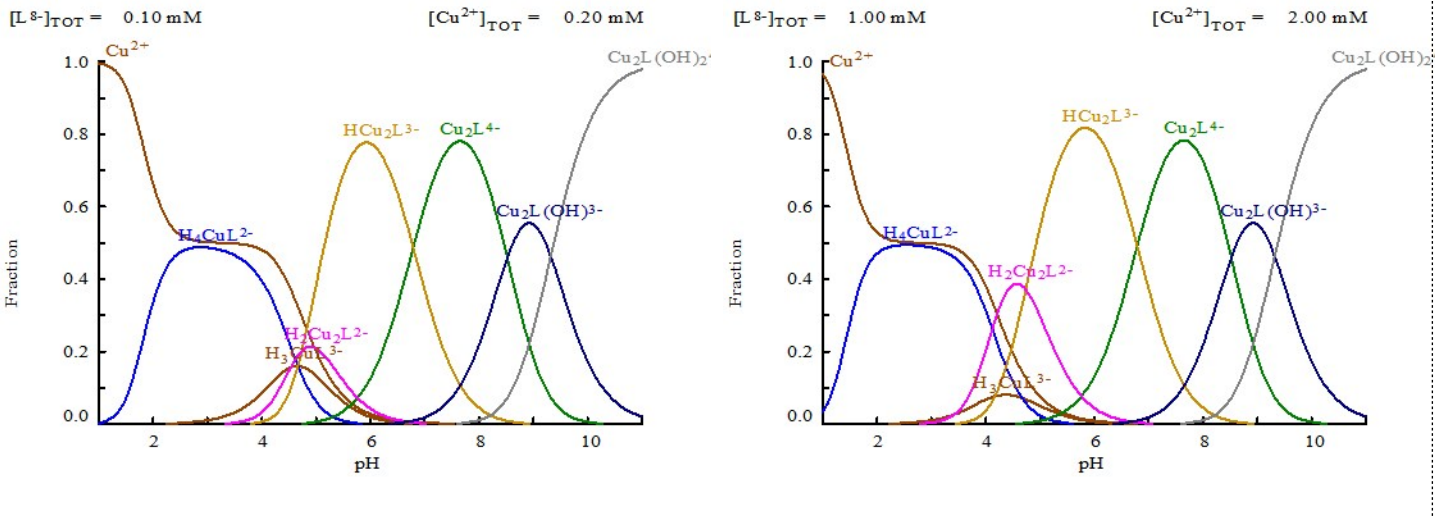


Figure S7: Distribution diagram for Cu^{2+} - H_8dotp system ($\text{Cu}:\text{L} = 2:1$) for lower (left) and higher (right) concentrations employed in the experiments.

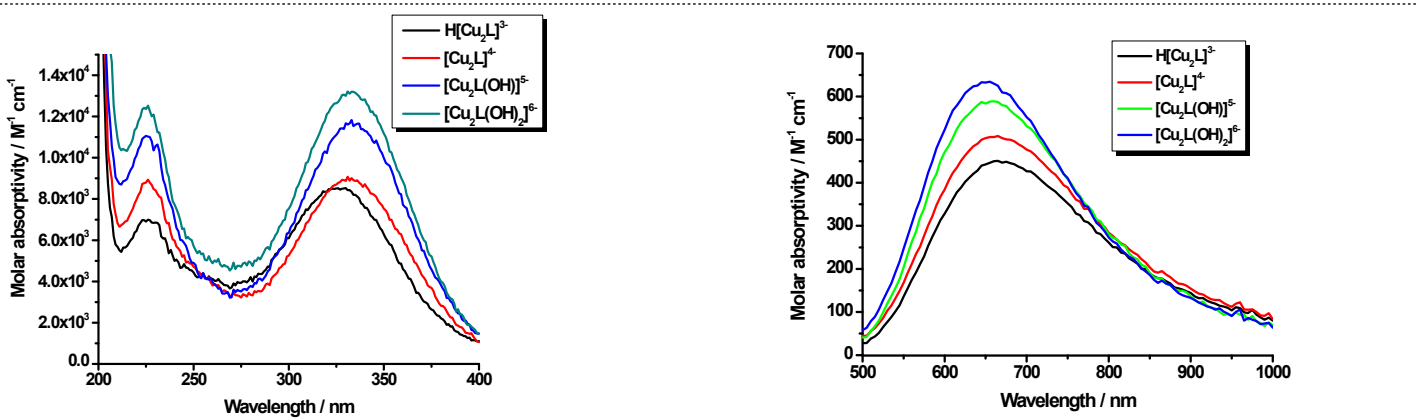


Figure S8: Calculated electronic spectra of dinuclear species in the Cu^{2+} - H_8dotp system measured in VIS (left; $c_L = 1.0$ mM, $c_{\text{Cu}} = 2.0$ mM) and UV (right; $c_L = 0.1$ mM, $c_{\text{Cu}} = 0.2$ mM) regions.

Table S1: UV-Vis spectral parameters calculated for species present in Cu(II)-DOTA-like ligand systems.

Ligand	Species	$\lambda_{\max} / \text{nm}$	$\epsilon_{\max} / \text{M}^{-1} \text{cm}^{-1}$
H₈dotp	[Cu(L)] ⁶⁻	648 358	670 6010
	[Cu(HL)] ⁵⁻	650 357	640 5660
	[Cu(H ₂ L)] ⁴⁻	648 352	575 5310
	[Cu(H ₃ L)] ³⁻	652 351	530 5650
	[Cu(H ₄ L)] ²⁻	628 351	630 5580
	[Cu ₂ (HL)] ³⁻	663 326 226	450 8520 7000
	[Cu ₂ (L)] ⁴⁻	663 328 226	510 8930 8940
	[Cu ₂ (L)(OH)] ⁵⁻	657 333 226	590 11830 11030
	[Cu ₂ (L)(OH) ₂] ⁶⁻	653 333 226	630 13200 12530
	[Cu(L)] ⁴⁻	648 357	390 5330
	[Cu(HL)] ³⁻	668 350 300 (sh)	235 3770 3250
	[Cu(H ₂ L)] ²⁻	748 292 345 (sh)	120 4060 2540
trans-H₆do2a2p	[Cu(H ₃ L)] ⁻	680 349	290 4500
	[Cu(L)] ²⁻	744 294 351 (sh)	100 4010 2360
	[Cu(HL)] ⁻	740 291	70 4740
	[Cu(H ₂ L)]	740 292	60 5000
H₄dota	[Cu(L)] ²⁻	744 294 351 (sh)	100 4010 2360
	[Cu(HL)] ⁻	740 291	70 4740
	[Cu(H ₂ L)]	740 292	60 5000

Table S2: Summary of stepwise protonation constants of the title ligands ($t = 25$ °C, $I = 0.1$ M (K/NMe₄)Cl).

Constant	<i>trans</i> -H ₂ do2a ^[1]	H ₄ dota ^[2,3]	H ₅ do3ap ^[4]	<i>trans</i> -H ₆ do2a2p ^[5,6]	H ₇ doa3p ^[7,8]	H ₈ dotp ^[9]	H₈dotp^c
log K_1	11.45	11.9	13.83	13.02	13.66 ^a <i>14.22^b</i>	14.65	—
log K_2	9.54	9.72	10.35	11.82	12.11 ^a <i>11.81^b</i>	12.40	12.75
log K_3	4.00	4.5	6.54	6.35	7.19 ^a <i>8.08^b</i>	9.28	9.20
log K_4	2.36	4.3	4.34	6.33	6.15 ^a <i>6.51^b</i>	8.09	8.01
log K_5	<2.3	2.36	3.09	3.13	5.38 ^b	6.12	6.03
log K_6	<2.3	—	1.63	2.64	2.86 ^b	5.22	5.18
log K_7	—	—	1.07	—	—	1.77	1.74
log $\beta_2 =$	20.99	21.62	24.18	24.84	26.03 ^b	27.05	27.40
log $K_1 + \log K_2$							

^aDetermined from ¹H and ³¹P NMR titrations; no control of the ionic strength, $t = 21.0$ °C.^[7]^bCalculated from the published^[8] overall protonation constants ($I = 1.0$ M KCl); in italics.^cThis work; in **bold**.**Table S3:** Summary of derived equilibrium constants for systems with Cu(II) ion and the title ligands ($t = 25$ °C, $I = 0.1$ M (K/NMe₄)Cl).

Equilibrium ^a	Ligand						H₈dotp^b
	Constant	<i>trans</i> -H ₂ do2a ^[1]	H ₄ dota ^[2,3]	<i>trans</i> -H ₆ do2a2p ^[5,6]	H ₇ doa3p ^[8]	H ₈ dotp ^[10,11]	
Cu + L \leftrightarrow [Cu(L)]	21.1	22.3	25.17	27.6 ^c	25.4	29.93	
log K_1 (CuL)	—	—	—	—	—	—	
[Cu(L)] + Cu \leftrightarrow [Cu ₂ (L)]	—	2.23	6.19	7.9 ^c	6.64	9.35	
log K_2 (Cu ₂ L)	—	—	—	—	—	—	
[Cu(HL)] \leftrightarrow [Cu(L)] + H	3.0	4.30	7.23	—	7.41	7.96	
p K_{a1} (CuHL)	—	—	—	—	—	—	
[Cu(H ₂ L)] \leftrightarrow [Cu(HL)] + H	—	3.55	6.66	—	6.42	7.20	
p K_{a2} (CuH ₂ L)	—	—	—	—	—	—	
[Cu(H ₃ L)] \leftrightarrow [Cu(H ₂ L)] + H	—	—	2.51	—	6.16	6.43	
p K_{a3} (CuH ₃ L)	—	—	—	—	—	—	
[Cu(H ₄ L)] \leftrightarrow [Cu(H ₃ L)] + H	—	—	—	—	4.58	4.67	
p K_{a4} (CuH ₄ L)	—	—	—	—	—	—	

^aCharges are omitted. ^bThis work; in **bold**. ^cEstimated from LFER plot at Figure S9 on the basis of the literature ligand protonation constants.

Table S4: Overall protonation constants of H₈dotp (β_h)^a and stability constants for the Cu(II)–H₈dotp system (β_{hlm})^b determined in this work ($t = 25^\circ\text{C}$, $I = 0.1 \text{ M}$ (NMe₄)Cl). The errors are standard deviations given directly by the fitting program.

Equilibrium ^c	Constant
L + H \leftrightarrow HL	log β_1
L + 2H \leftrightarrow H ₂ L	log β_2
L + 3H \leftrightarrow H ₃ L	log β_3
L + 4H \leftrightarrow H ₄ L	log β_4
L + 5H \leftrightarrow H ₅ L	log β_5
L + 6H \leftrightarrow H ₆ L	log β_6
L + 7H \leftrightarrow H ₇ L	log β_7
Cu + L \leftrightarrow [Cu(L)]	log β_{011}
Cu + L + H \leftrightarrow [Cu(HL)]	log β_{111}
Cu + L + 2H \leftrightarrow [Cu(H ₂ L)]	log β_{211}
Cu + L + 3H \leftrightarrow [Cu(H ₃ L)]	log β_{311}
Cu + L + 4H \leftrightarrow [Cu(H ₄ L)]	log β_{411}
2Cu + L \leftrightarrow [Cu ₂ (L)]	log β_{012}
2Cu + L + H \leftrightarrow [Cu ₂ (HL)]	log β_{112}
2Cu + L + 2H \leftrightarrow [Cu ₂ (H ₂ L)]	log β_{212}
2Cu + L + H ₂ O \leftrightarrow [Cu ₂ (L)(OH)] + H	log β_{-112}
2Cu + L + 2H ₂ O \leftrightarrow [Cu ₂ (L)(OH) ₂] + 2H	log β_{-212}

^a $\beta_h = [\text{H}_h\text{L}] / [\text{L}] \cdot [\text{H}]^h$; charges are omitted. ^b $\beta_{hlm} = [\text{H}_h\text{LCu}_m] / [\text{L}] \cdot [\text{H}]^h \cdot [\text{Cu}]^m$, $l = 1$; charges are omitted. ^cCharges are omitted.

Table S5: Full set of derived equilibrium constants for the Cu(II)–H₈dotp system ($t = 25^\circ\text{C}$, $I = 0.1 \text{ M}$ (NMe₄)Cl).

Equilibrium ^a	Constant		
Cu + L \leftrightarrow [Cu(L)]	log $K_1(\text{CuL})$	29.93	25.4 ^b
[Cu(HL)] \leftrightarrow [Cu(L)] + H	p $K_{a1}(\text{CuHL})$	7.96	7.41 ^b
[Cu(H ₂ L)] \leftrightarrow [Cu(HL)] + H	p $K_{a2}(\text{CuH}_2\text{L})$	7.20	7.16 ^b
[Cu(H ₃ L)] \leftrightarrow [Cu(H ₂ L)] + H	p $K_{a3}(\text{CuH}_3\text{L})$	6.43	6.42 ^b
[Cu(H ₄ L)] \leftrightarrow [Cu(H ₃ L)] + H	p $K_{a4}(\text{CuH}_4\text{L})$	4.67	4.58 ^b
[Cu(L)] + Cu \leftrightarrow [Cu ₂ (L)]	log $K_2(\text{Cu}_2\text{L})$	9.35	6.64 ^b
[Cu(HL)] + Cu \leftrightarrow [Cu ₂ (HL)]	log $K_2(\text{Cu}_2\text{HL})$	8.18	5.82 ^b
[Cu(H ₂ L)] + Cu \leftrightarrow [Cu ₂ (H ₂ L)]	log $K_2(\text{Cu}_2\text{H}_2\text{L})$	5.72	
[Cu ₂ (HL)] \leftrightarrow [Cu ₂ (L)] + H	p $K_{a21}(\text{Cu}_2\text{HL})$	6.79	
[Cu ₂ (H ₂ L)] \leftrightarrow [Cu ₂ (HL)] + H	p $K_{a22}(\text{Cu}_2\text{H}_2\text{L})$	4.74	
[Cu ₂ (L)] + H ₂ O \leftrightarrow [Cu ₂ (L)(OH)] + H	p $K_{a1\text{OH}}(\text{Cu}_2\text{L})$	8.52	
[Cu ₂ (L)(OH)] + H ₂ O \leftrightarrow [Cu ₂ (L)(OH) ₂] + H	p $K_{a2\text{OH}}(\text{Cu}_2\text{L})$	9.4	

^aCharges are omitted. ^bRef.^[10,11].

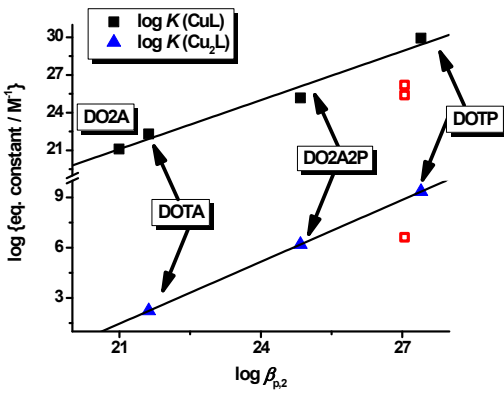


Figure S9: Correlation of values of stability constant for copper(II) mononuclear and dinuclear complexes with basicity of macrocyclic ring represented by overall protonation constant $\log\beta_2 = \log K_1 + \log K_2$. The red points are experimental data for the Cu(II)-H₈dotp system taken from literature.^[10,11,12]

The solid lines representing Linear Free Energy Relationship (LFER) plots calculated with the literature (*trans*-H₂do2a, H₄dotra, *trans*-H₆do2a2p) and measured (H₈dotp) data give correlations $\log K_{\text{CuL}} = 1.3 \times \log\beta_2 - 6.2$ and $\log K_{\text{Cu2L}} = 1.2 \times \log\beta_{p,2} - 24.4$ for the mono- and dinuclear copper(II) complexes, respectively. As it can be seen, there is a discrepancy in stability constant values published by Kabachnik et al.^[10,11] and Martell et al.^[12] for the [Cu(dotp)]⁶⁻ and [Cu₂(dotp)]⁴⁻ complexes which are underestimated about three orders of magnitude. On the other hand, the values obtained in this paper are in agreement with the stability constant values expected from this LFER plot. Thus, this plot can be also utilized for prediction of unpublished $\log K_{\text{CuL}}$ values for the other copper(II) complexes - *e.g.* values of $\log K_{\text{CuL}}$ and $\log K_{\text{Cu2L}}$ for H₇doa3p could be estimated to be 27.6 and 7.9 (the experimental values $\log K_{\text{CuL}} = 27.3$ and $\log K_{\text{Cu2L}} = 5.91$ were determined for $T = 298.2$ K and $I = 1.0$ M KCl – see ref.^[8]); they are similar to those for Cu(II)-H₈dotp complexes as ligands have similar basicity and structures of the complex are probably similar. In addition, $\log K_{\text{Cu2L}} \sim 6.9$ for the H₇doa3p complex estimated from formation kinetics data (see below, Figure S22) is in a good agreement with the estimate from the plot - it cross-validates our results obtained from both thermodynamic and kinetic studies.

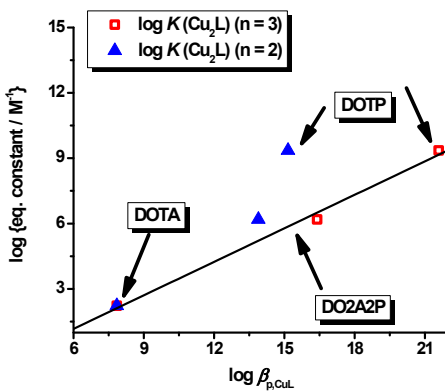


Figure S10: Correlation of values of stability constant for copper(II) dinuclear complexes with basicity of pendant arms in the copper(II) mononuclear complex represented by overall protonation constant $\log\beta_{pn}$. The blue and red points represent correlations with $\log\beta_{p2} = \log K_{p1}(\text{CuL}) + \log K_{p2}(\text{CuHL})$ and $\log\beta_{p3} = \log K_{p1}(\text{CuL}) + \log K_{p2}(\text{CuHL}) + \log K_{p3}(\text{CuH}_2\text{L})$, respectively.

Potentiometry on H₈dotp and the Cu(II)-H₈dotp system

Experimental:

Potentiometry was carried out according to the previously published procedure^[13] Briefly, (NMe₄)Cl (Fluka) was recrystallized from boiling *i*-PrOH; (NMe₄)OH stock solution (~0.2 M) was prepared from the (NMe₄)Cl on anion exchanger (Dowex 1 in OH⁻ form, Fluka) and its concentration was determined with potassium hydrogenphthalate; HCl stock solutions (0.03 M and 0.2 M) were prepared from conc. aq. HCl (Merck, trace analysis) and their concentrations were determined against the (NMe₄)OH stock solution; deionized water was used; argon saturated with water vapour was used as protecting gas against air CO₂; stock solution of Cu²⁺ was prepared from recrystallized CuCl₂ hydrate (Lachema) and its concentration was determined by chelatometry. Exact concentration of the H₈dotp stock solution was determined together with fitting of the protonation constants and agreed well with that determined by weight of the dried (80 °C, 2 h) solid ligand sample. Combined electrode (GK 2401B, Radiometer) was calibrated by acid-base titration in the same pH ranges as titrations below. The 2-ml autoburette ABU 901 and pH-meter PHM 240 (both Radiometer) were used to deliver the hydroxide solution and to measure potential, respectively. The titration data were treated with OPIUM program package^[14] The program minimizes the criterion of the generalised least-squares method using the calibration function $E = E_0 + S \times \log[H^+] + j_1 \times [H^+] + j_2 \times K_w/[H^+]$ where the additive term E_0 contains the standard potentials of the electrodes used and contributions of inert ions to the liquid junction potential, S corresponds to the Nernstian slope, the value of which should be close to the theoretical value, and $j_1 \times [H^+]$ and $j_2 \times K_w/[H^+] = j_2 \times [OH^-]$ terms are the contributions of the H⁺ and OH⁻ ions to the liquid-junction potential. It is clear that j_1 and j_2 cause deviation from a linear dependence of E on $-\log[H^+]$ only in strongly acidic and strongly alkaline solutions. The calibration parameters were determined by titration of standard HCl with standard (Me₄N)OH solutions before each ligand or ligand–metal titration to give a pair calibration/titration which was used for calculations of the constants.

All constants were determined in 0.1 M NMe₄Cl at 25.0 ± 0.1 °C with pK_w = 13.81. The H₈dotp ($c_L = 0.004$ M) for protonation constant determination was titrated in pH range 1.5–12.2, four independent titrations and ~50 points per titration. Copper(II)–H₈dotp system was titrated in 1 : 1 ($c_L = c_{Cu} = 0.004$ M, pH range 1.4–11.9) and 1 : 2 ($c_L = 0.004$ M, $c_{Cu} = 0.008$ M, pH range 1.4–9, copper(II) hydroxide precipitated at pH > 9) ligand-to-metal molar ratios, at least three independent titrations, ~60 (1 : 1) or ~40 (1 : 2) points per titration. Equilibrium was established immediately except pH range ~3.5 – ~7.5 in L : Cu = 1 : 2 ratio where waiting time was up to 2.5 min per titration point. Throughout the paper, pH means $-\log[H^+]$. The calculated constants are concentration constants defined as $\beta_{hlm} = [H_h L_l M_m] / [H]^h \cdot [L]^l \cdot [M]^m$ and the standard deviations are given directly by the program. The water ion product pK_w (13.81) and stability constants of the Cu²⁺–OH⁻ systems included in the calculation were taken from literature.^[15,16] Value of the first protonation constant of H₈dotp ($\log\beta_1 = \log K_1 = 14.65$) is not accessible by potentiometric titrations and was taken from literature.^[9b]

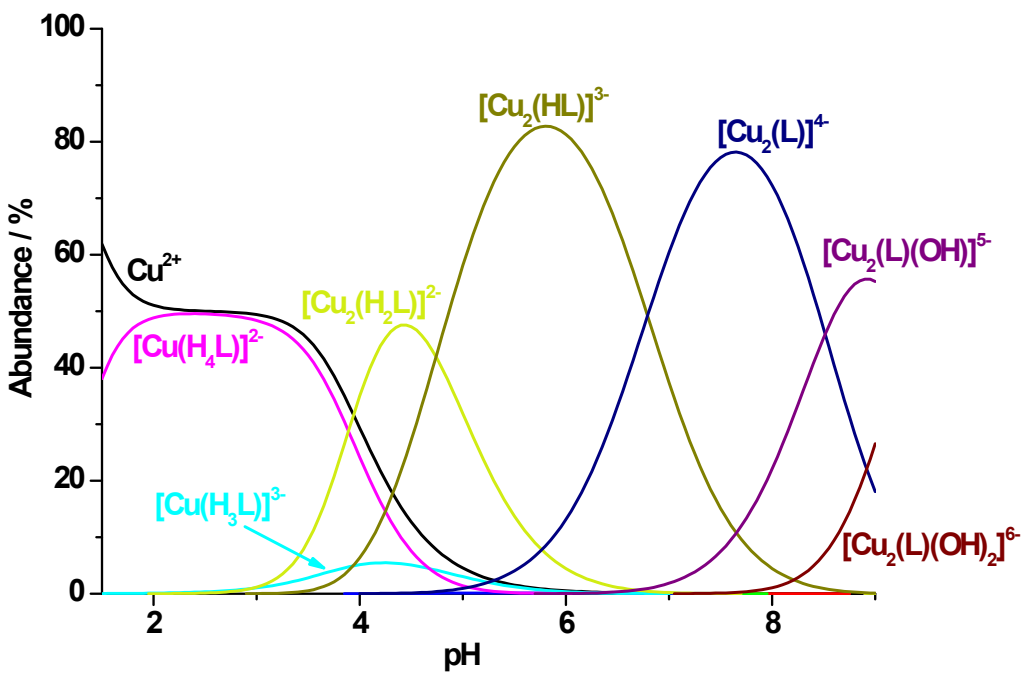
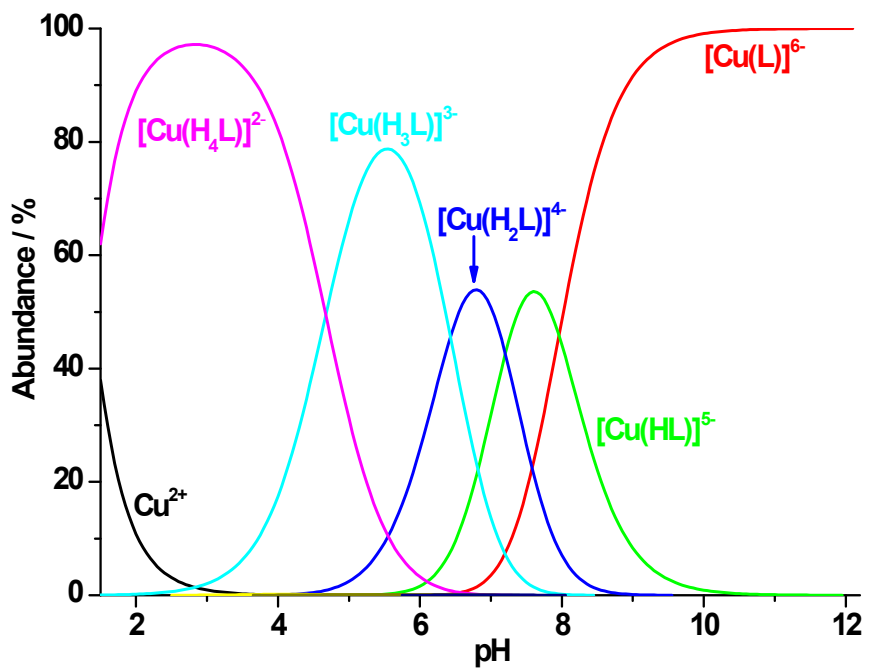


Figure S11: Distribution diagrams of the Cu(II)-H₈dotp system for L : Cu 1 : 1 molar ratio (upper, $c_{\text{L}} = c_{\text{Cu}} = 0.004 \text{ M}$), and for L : Cu 1 : 2 molar ratio (lower, $c_{\text{L}} = 0.004 \text{ M}$, $c_{\text{Cu}} = 0.008 \text{ M}$).

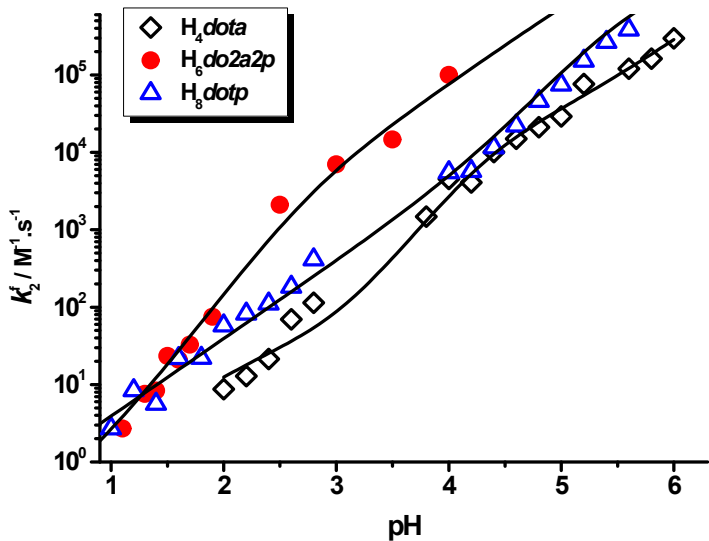


Figure S12: Dependence of the second-order formation rate constants, f_k_2 , for the copper(II) complexes with $H_4\text{dot}\text{a}$ (\diamond), *trans*- $H_6\text{do}2\text{a}2\text{p}$ (\bullet) and $H_8\text{dot}\text{p}$ (Δ) on pH; the full-line curves were fitted through the experimental data according to Equation 1 with parameters given in Table 1.

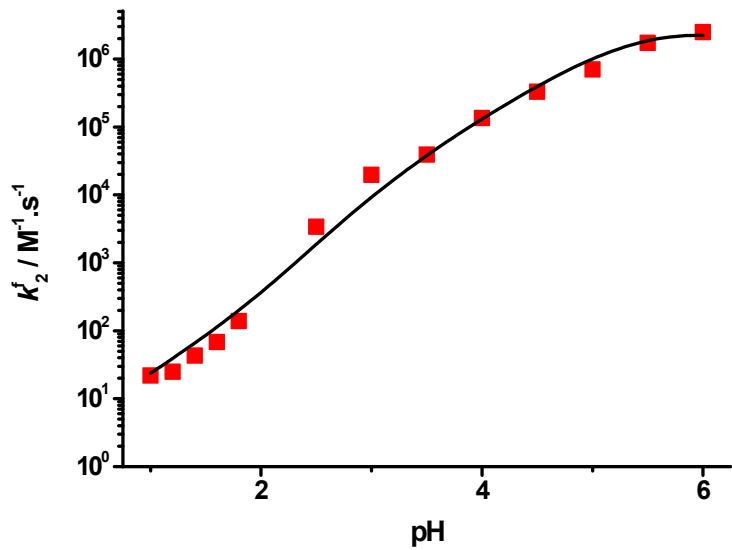


Figure S13: Dependence of the second-order formation rate constants, f_k_2 , for the copper(II) complexes with $H_7\text{do}a3\text{p}$ on pH; the full-line curve was fitted through the experimental data according to Equation 1 with parameters given in Table 1.

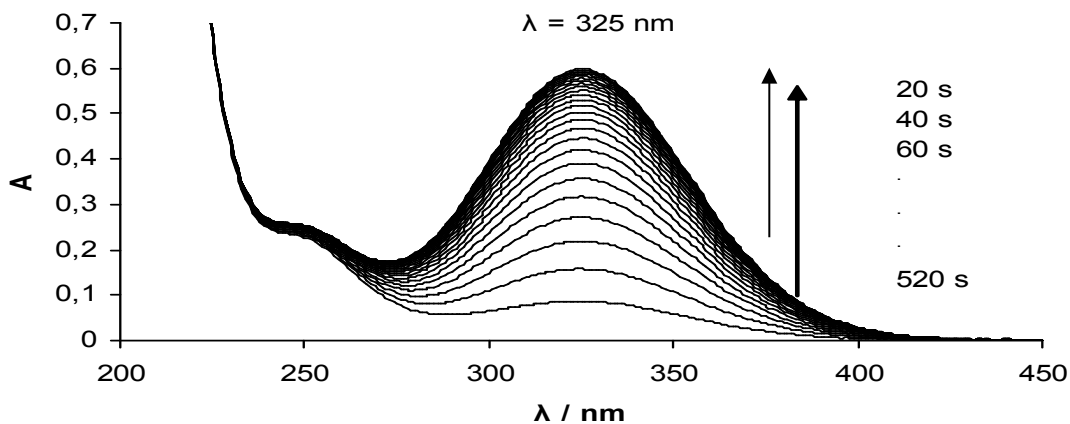


Figure S14: Example of time change of absorption spectra in the course of formation of the $[\text{Cu}(\text{dotp})]^{6-}$ complex ($c_{\text{L}} = 1 \times 10^{-4}$ M, $c_{\text{Cu}} = 1 \times 10^{-3}$ M; pH 1.4; $I = 0.1$ M KCl; $T = 298.2$ K).

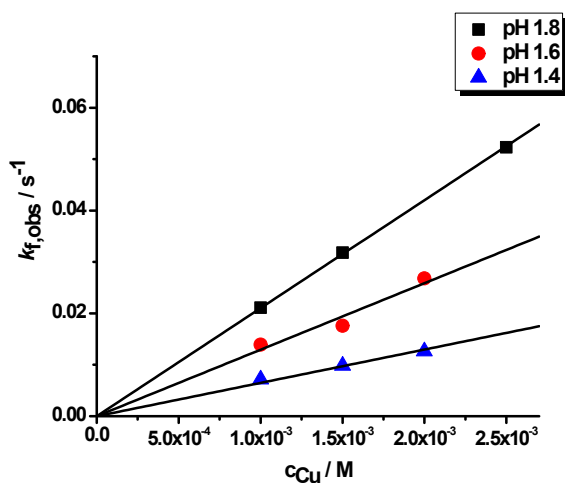


Figure S15: Dependence of pseudo-first order rate constant on copper(II) ion concentration for formation of the $[\text{Cu}(\text{dotp})]^{6-}$ complex ($c_{\text{L}} = 1 \times 10^{-4}$ M, $I = 0.1$ M KCl; $T = 298.2$ K).

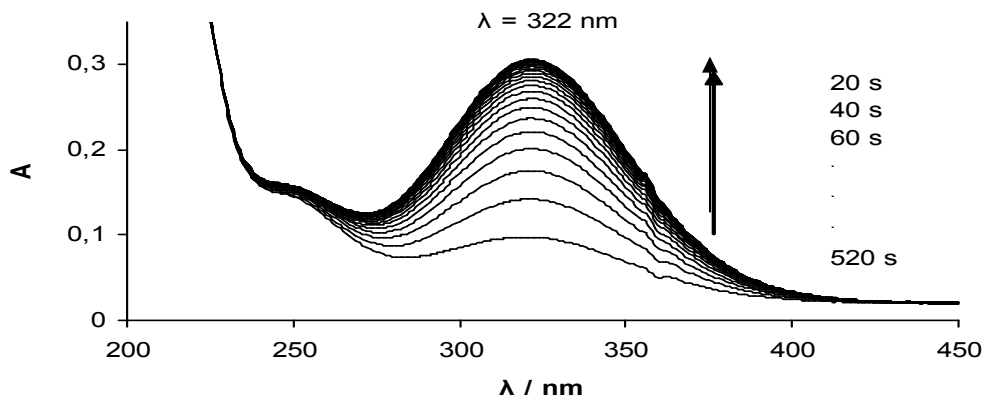


Figure S16: Example of time change of absorption spectra in the course of formation of the $[\text{Cu}(\text{doa3p})]^{5-}$ complex ($c_{\text{L}} = 5 \times 10^{-5}$ M, $c_{\text{Cu}} = 5 \times 10^{-4}$ M; pH 1.4; $I = 0.1$ M KCl; $T = 298.2$ K).

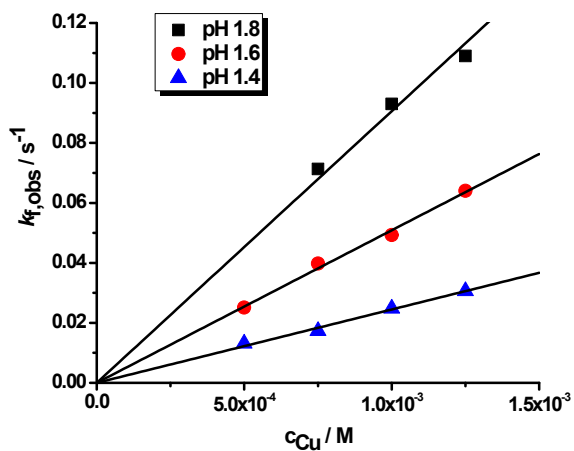


Figure S17: Dependence of pseudo-first order rate constant on copper(II) ion concentration for formation of the $[\text{Cu}(\text{doa3p})]^{5-}$ complex ($c_{\text{L}} = 5 \times 10^{-5}$ M, $I = 0.1$ M KCl; $T = 298.2$ K).

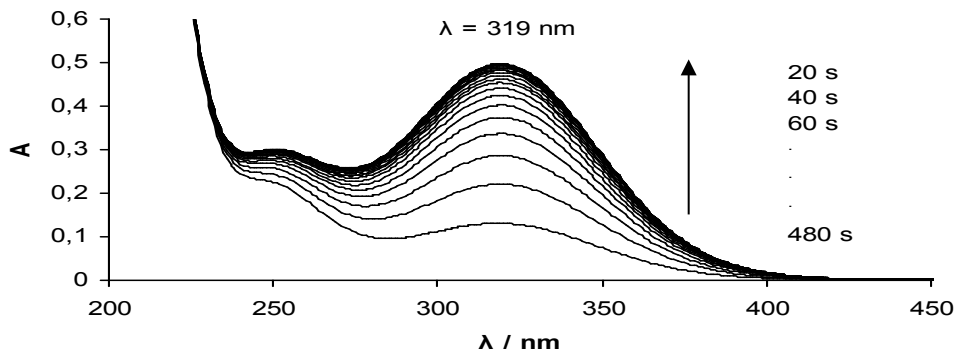


Figure S18: Example of time change of absorption spectra in the course of formation of the $[\text{Cu}(\text{trans}-\text{do}2\text{a}2\text{p})]^{4-}$ complex ($c_L = 1 \times 10^{-4}$ M, $c_{\text{Cu}} = 1 \times 10^{-3}$ M; pH 1.4; $I = 0.1$ M KCl; $T = 298.2$ K).

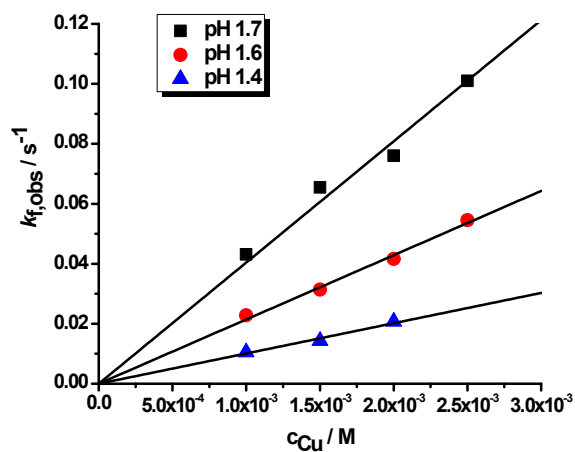


Figure S19: Dependence of pseudo-first order rate constant on copper(II) ion concentration for formation of the $[\text{Cu}(\text{trans}-\text{do}2\text{a}2\text{p})]^{4-}$ complex ($c_L = 1 \times 10^{-4}$ M, $I = 0.1$ M KCl; $T = 298.2$ K).

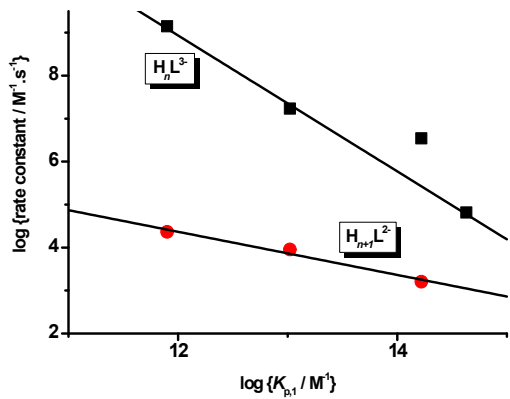


Figure S20: LFER plot showing correlation of partial rate constants of formation of Cu(II) complexes for triple charged species (■, k_{HL} for H_4dota , k_{H3L} for *trans*- $\text{H}_6\text{do2a2p}$, k_{H4L} for $\text{H}_7\text{doa3p}$, k_{H5L} for H_8dotp) and double charged (●, k_{H2L} for H_4dota , k_{H4L} for *trans*- $\text{H}_6\text{do2a2p}$, k_{H5L} for $\text{H}_7\text{doa3p}$) species with the first protonation constants of the ligands. The experimental conditions are given in the Experimental.

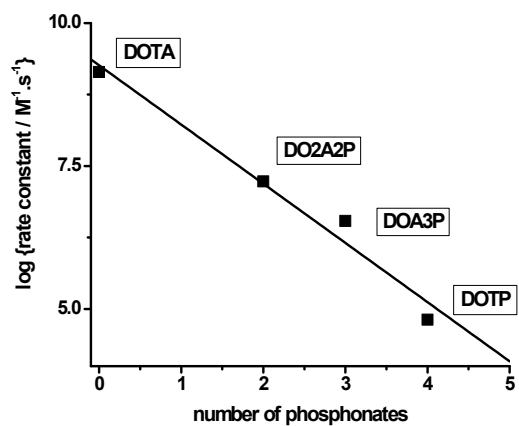


Figure S21: Dependence of rate constants for reaction of triple-charged species of the ligands with Cu(II) on a number of phosphonic acid groups ($T = 298.2 \text{ K}$).

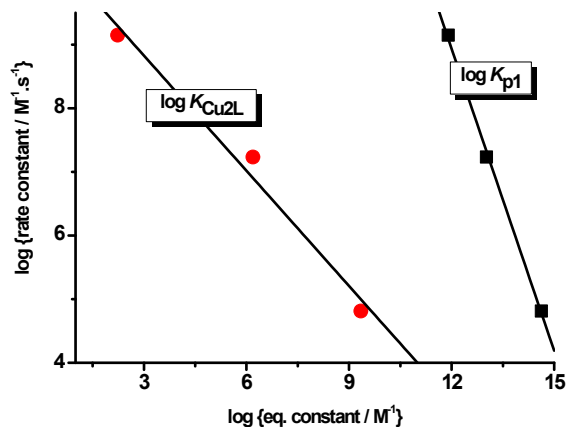


Figure S22: LFER plot showing correlation of partial rate constants (for triply negative species) for formation of copper(II) complexes of H_4dota (k_{HL}), *trans*- $\text{H}_6\text{do2a2p}$ (k_{H3L}) and H_8dotp (k_{H5L}).

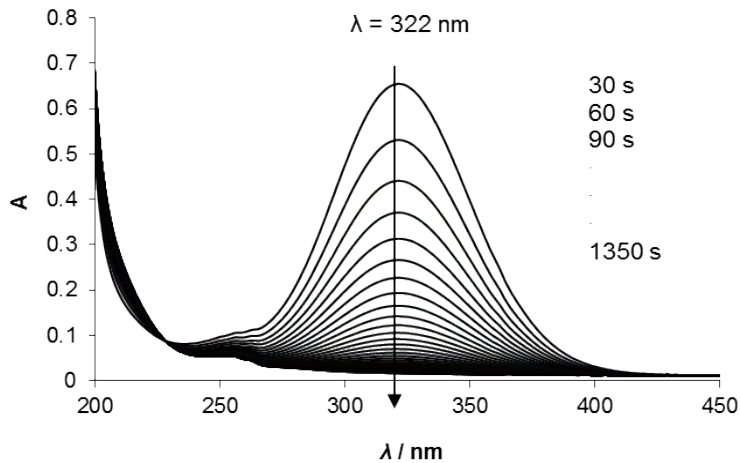


Figure S23: Time change in the absorption spectra in the course of decomplexation of the $[\text{Cu}(\text{dotp})]^{6-}$ complex ($c_{\text{CuL}} = 1 \times 10^{-4}$ M; $[\text{H}^+] = 5.00$ M; $I = 5.00$ M ($\text{H}_3\text{Na}\text{ClO}_4$); $T = 288.2$ K).

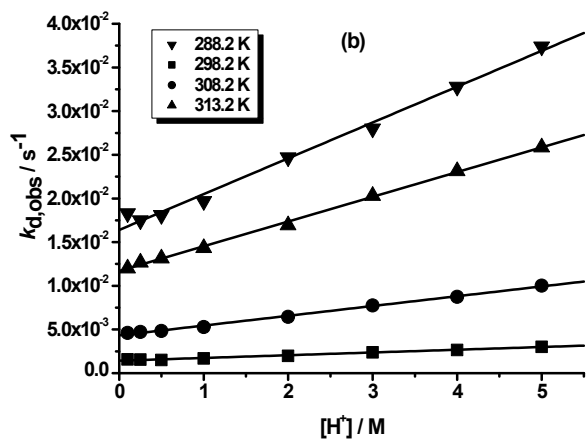


Figure S24: Pseudo-first order rate constants as function of proton concentration for acid-assisted decomplexation of the $[\text{Cu}(\text{dotp})]^{6-}$ complex ($I = 5.0$ M ($\text{Na}_3\text{H}\text{ClO}_4$)).

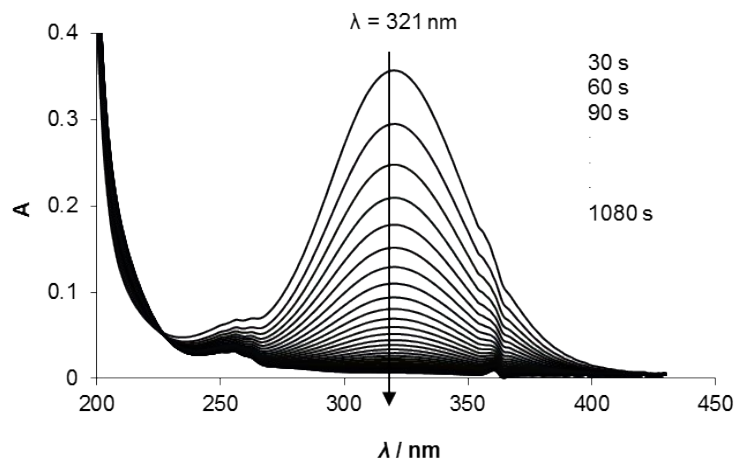


Figure S25: Time change in the absorption spectra in the course of decomplexation of the $[\text{Cu}(\text{doa3p})]^{5-}$ ($c_{\text{CuL}} = 5 \times 10^{-5}$ M; $[\text{H}^+] = 5.00$ M; $I = 5.00$ M ($\text{H}_3\text{Na}\text{ClO}_4$; $T = 298.2$ K).

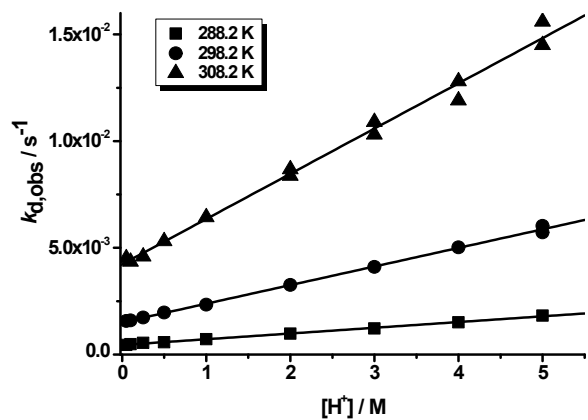


Figure S26: Pseudo-first order rate constants as function of proton concentration for acid-assisted decomplexation of the $[\text{Cu}(\text{doa3p})]^{5-}$ complex ($I = 5.0$ M ($\text{Na}_3\text{H}\text{ClO}_4$).

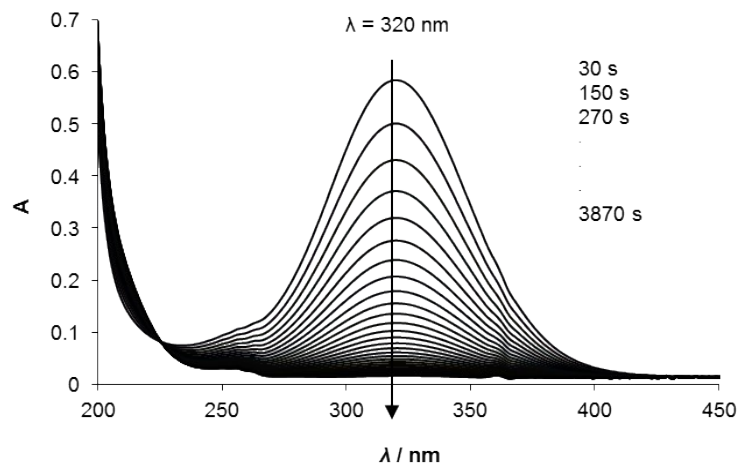


Figure S27: Time change in the absorption spectra in the course of decomplexation of the $[\text{Cu}(\text{trans}-\text{do}2\text{a}2\text{p})]^{4-}$ complex ($c_{\text{CuL}} = 1 \times 10^{-4} \text{ M}$; $[\text{H}^+] = 5.00 \text{ M}$; $I = 5.00 \text{ M}$ ($\text{H}_3\text{Na}\text{ClO}_4$); $T = 298.2 \text{ K}$).

Table S5. Kinetic parameters for acid-assisted decomplexation of Cu(II) complexes of studied ligands ($I = 5.0 \text{ M} (\text{Na}_2\text{HClO}_4)$).

Ligand	Temperature (K)				ΔH^\ddagger (kJ mol $^{-1}$)	ΔS^\ddagger (J mol $^{-1}$ K $^{-1}$)
Rate Constant	288.2	298.2	308.2	313.2		
H₈dotp	288.2	298.2	308.2	313.2		
$k_1 / 10^{-3}, \text{s}^{-1}$	1.43(4)	4.33(7)	11.7(1)	16.4(9)	72(3)	-50(9)
$k_2 / 10^{-3}, \text{M}^{-1} \text{s}^{-1}$	0.31(1)	1.12((3))	2.83(5)	4.1(3)	75(5)	-50(16)
$k_2 / k_1, \text{M}^{-1}$	0.21(1)	0.26(1)	0.242(5)	0.25(2)		
H₇doa3p	288.2	298.2	308.2			
$k_1 / 10^{-3}, \text{s}^{-1}$	0.45(1)	1.51(4)	4.2(2)		80(2)	-32(8)
$k_2 / 10^{-3}, \text{M}^{-1} \text{s}^{-1}$	0.267(4)	0.87(1)	2.13(1)		74(5)	-55(16)
$k_2 / k_1, \text{M}^{-1}$	0.59(2)	0.58(2)	0.51(2)			
trans-H₆do2a2p	298.2	313.2	323.2	333.2		
$k_1 / 10^{-3} \text{ s}^{-1}$	0.411(8)	1.90(7)	4.52(8)	10.2(4)	73(1)	-64(4)
$k_2 / 10^{-3} \text{ M}^{-1} \text{ s}^{-1}$	0.173(3)	0.69(3)	1.44(4)	2.6(1) $\times 10^{-3}$	62(3)	-110(10)
$k_2 / k_1, \text{M}^{-1}$	0.42(1)	0.36(2)	0.32(1)	0.25(1)		
H₅do3ap^[17]	298.2	313.2	323.2			
$k_1 / 10^{-5}, \text{s}^{-1}$	7.84	28.8	67.6		66	-101
$k_2 / 10^{-5}, \text{M}^{-1} \text{s}^{-1}$	0.43	3.3	12.3		105	-3
$k_2 / k_1, \text{M}^{-1}$	0.055	0.115	0.181			
H₄dota^[17]	298.2	318.2	328.2	338.2		
$k_1 / 10^{-5}, \text{s}^{-1}$	0.584 ^a	3.4	6.3	15.6	65	-128
$k_2 / 10^{-5}, \text{M}^{-1} \text{s}^{-1}$	0.0206 ^a	0.3	1.4	3.5	107	-15
$k_2 / k_1, \text{M}^{-1}$	0.035	0.088	0.222	0.222		
trans-H₂do2a^b	298.2	323.2	333.2	343.2		
$k_1 / 10^{-5}, \text{s}^{-1}$	0.605 ^a	5.3(1)	12.9(4)	24.6(9)	68(5)	-117(16)
$k_2 / 10^{-5}, \text{M}^{-1} \text{s}^{-1}$	0.0563 ^a	0.72(3)	1.7(1)	4.2(3)	78(2)	-102(6)
$k_2 / k_1, \text{M}^{-1}$	0.093	0.135(6)	0.133(9)	0.170(13)		
K / M^{-1}	22 ^a	19(1)	13(2)	16(2)	-8(15)	2(46)

^aExtrapolated from temperature dependence using activation/thermodynamic parameters.

^bFitted to the equation $k_{d,\text{obs}} = \frac{k_1 \times K \times [\text{H}^+] + k_2 \times K \times [\text{H}^+]^2}{1 + K \times [\text{H}^+]} = \frac{K \times [\text{H}^+] (k_1 + k_2 \times [\text{H}^+])}{1 + K \times [\text{H}^+]}$

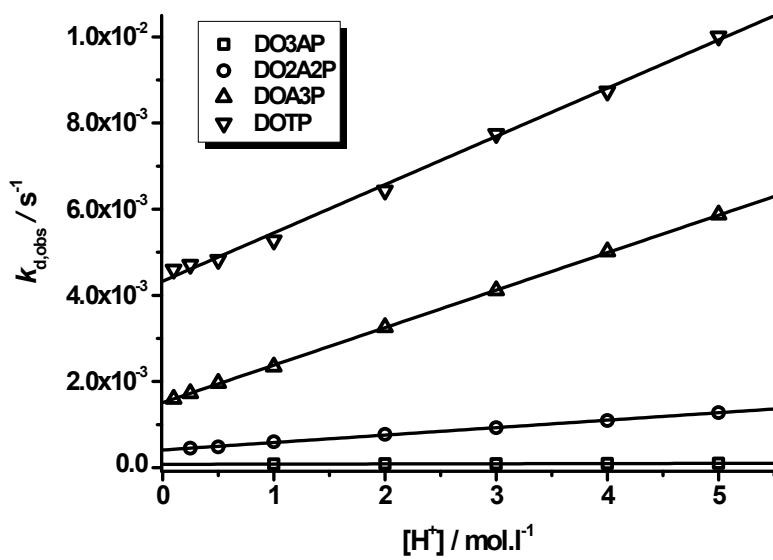


Figure S28: Dependence of rate constants for acid-assisted dissociation of Cu(II) complexes of H₄dota and its analogues on proton concentration obtained ($T = 298.2$ K). The experimental data for H₃do3a and H₅do3ap were taken from ref.^[17]

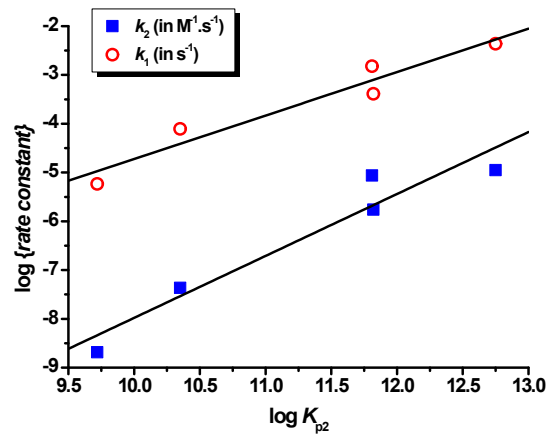


Figure S29: Dependence of rate constants for acid-assisted dissociation of the Cu(II) complexes on basicity of the ring nitrogen atoms expressed as sum of first two ligand protonation constants.

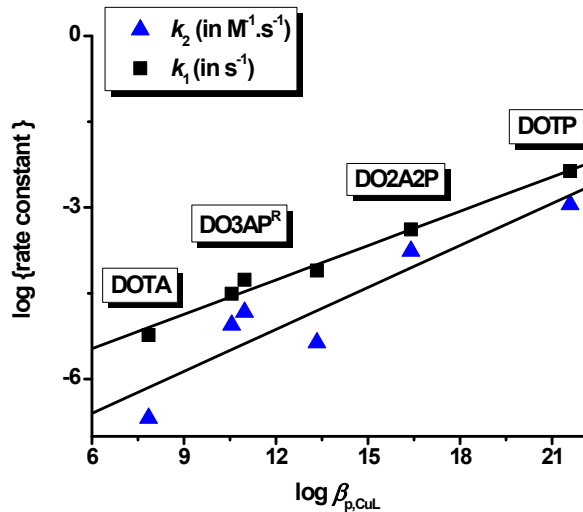
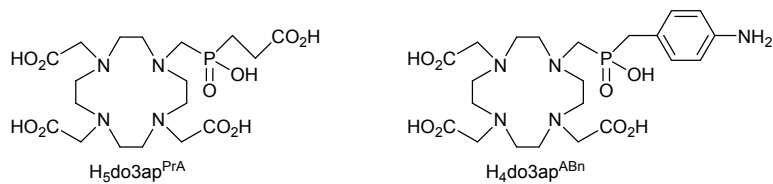


Figure S30: Correlation of rate constants for acid-assisted dissociation of Cu(II) complexes with basicity of pendant arms of the Cu(II) complexes represented by overall protonation constant: $\log \beta_{p3}(\text{CuL}) = \log K_{p1}(\text{CuL}) + \log K_{p2}(\text{CuHL}) + \log K_{p3}(\text{CuH}_2\text{L})$.

The solid lines representing Linear Free Energy Relationship (LFER) plots give correlation $\log k_1 = 0.20 \times \log \beta_{p,CuL} - 6.67$ and $\log k_2 = 0.25 \times \log \beta_{p,CuL} - 8.07$. The experimental kinetic data are obtained from Table 3 and from ref. [17]. The protonation constants for $\log \beta_{p3}(\text{CuL})$ for H₅do3ap (13.34) and monophosphinate ligands, H₅do3ap^{PrA} (10.98) and H₄do3ap^{ABn} (10.56), were obtained from literature (M. Málková, *PhD Thesis*, Charles University in Prague, Prague 2009). Thus, this plot can be also utilized for prediction of unpublished $\log K_{CuL}$ values for the other copper(II) complexes - *e.g.* values of $\log \beta_{p3}(\text{CuL})$ for the Cu(II)-H₇doa3p complex could be estimated as 19.3 and 20.5 (the experimental value $\log \beta_{p3}(\text{CuL}) = 18.42$ was determined for $T = 298.2 \text{ K}$ and $I = 1.0 \text{ M KCl}$ – see ref.[8]); they are similar to those for the Cu(II)-H₈dotp complex as both ligands have similar basicity and structures of their complexes are probably similar. Both previous values for the Cu(II)-H₇doa3p complex are in a good agreement and it can be also utilized as cross-validation of our results obtained from both thermodynamic and kinetic studies.



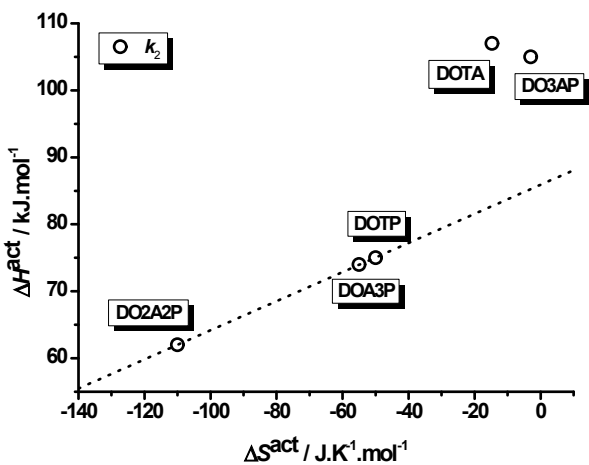
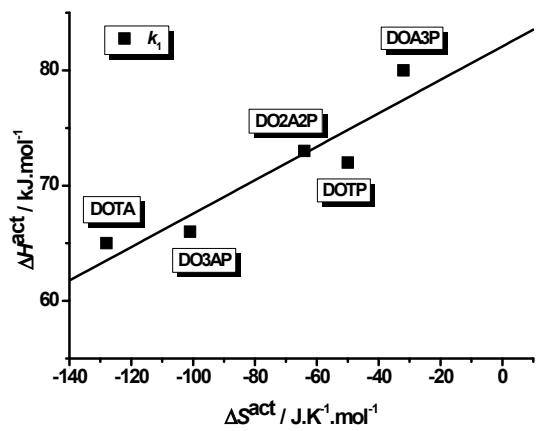


Figure S31: Isokinetic plots for Cu(II) complex dissociation.

Table S6: Experimental data for determination of crystal structure of KH₆doa3p·3H₂O (CCDC 1469446).

Parameter	KH ₆ do3ap·3H ₂ O
Formula	C ₁₃ H ₃₆ KN ₄ O ₁₄ P ₃
<i>M</i>	604.47
<i>T</i> , K	150(2) K
Crystal dimension, mm	0.24 × 0.20 × 0.16
Crystal system, Space group	Monoclinic, <i>C</i> 2/c (no. 15)
<i>a</i> , Å	37.6442(6)
<i>b</i> , Å	8.4336(1)
<i>c</i> , Å	16.1400(3)
β, °	110.457(1)
<i>U</i> , Å ³	4800.91(13)
<i>Z</i> ; <i>D</i> _c , g cm ⁻³	8; 1.673 Mg/m ³
λ, Å	0.71073
μ, mm ⁻¹	0.497
<i>F</i> (000)	2544
θ range of data collection, °	3.28 to 25.03
Index ranges	44 ≤ <i>h</i> ≤ 44, -10 ≤ <i>k</i> ≤ 10, -19 ≤ <i>l</i> ≤ 19
Data; restraints; parameters	4185; 0; 319
GOF on <i>F</i> ²	1.063
w <i>R</i> ^{a,b}	<i>R</i> ₁ = 0.0382, w <i>R</i> ₂ = 0.0993
Final <i>R</i> , <i>R'</i> indices [<i>I</i> > 2σ(<i>I</i>)]	<i>R</i> ₁ = 0.0461, w <i>R</i> ₂ = 0.1027
Largest difference peak and hole, e Å ⁻³	1.026 and -0.512

^a*w* = 1/[σ²(*F*₀²) + (*A*×*P*)² + *B*×*P*]; where *P* = (*F*₀² + 2*F*_c²) / 3 (SHELXL97, ref.^[18]).^b*R*₁ = Σ |*F*₀ - *F*_c| / Σ |*F*_c|; w*R*₂ = [Σ*w*(*F*₀² - *F*_c²)² / Σ*w*(*F*₀²)²]^{1/2} (SHELXL97, ref.^[18])

Table S7 Selected bond length and angles of the KH₆doa3p·3H₂O in the solid state.

Bond distances (Å)		Bond angles (°)			
N4–C14	1.511(4)	O1-P1-O2	107.36(11)	O5-C15-O4	126.2(3)
N1–C13	1.478(3)	O1-P1-O3	112.20(11)	O5-C15-C14	123.7(3)
N7–C16	1.483(4)	O2-P1-O3	113.12(11)	O4-C15-C14	109.3(2)
N10–C17	1.508(3)	O6-P2-O7	106.56(12)	N4-C14-C15	113.8(2)
C14–C15	1.541(4)	O6-P2-O8	110.95(11)	N1-C13-P1	114.7(2)
C15–O4	1.313(3)	O7-P2-O8	115.89(11)	N7-C16-P2	110.5(2)
C15–O5	1.208(3)	O9-P3-O10	109.70(11)	N10-C17-P3	116.2(2)
P1–O1	1.5510(19)	O9-P3-O11	108.24(11)	O1-P1-C13	106.93(12)
P1–O2	1.532(2)	O10-P3-O11	118.45(13)	O2-P1-C13	105.82(11)
P1–O3	1.5036(19)			O3-P1-C13	111.00(12)
P2–O6	1.5907(19)			O6-P2-C16	105.43(13)
P2–O7	1.5143(19)			O7-P2-C16	107.14(12)
P2–O8	1.4960(19)			O8-P2-C16	110.34(12)
P3–O9	1.591(2)			O9-P3-C17	102.70(12)
P3–O10	1.483(2)			O10-P3-C17	106.95(12)
P3–O11	1.480(2)			O11-P3-C17	109.57(12)
P1–C13	1.808(3)				
P2–C16	1.798(3)				
P3–C17	1.818(3)				
Hydrogen bond parameters					
O1–H1…O7	2.509(3)	O1-H1-O7	162.0		
N10–H10…O7	2.932(3)	N10-H10-O7	145.0		
N10–H10…N7	2.838(3)	N10-H10-N7	114.0		

N10—H10…N1	3.086(3)	N10-H10-N1	107.0
N4—H40…N1	3.027(3)	N4-H40-N1	109.0
N4—H40…N7	2.986(3)	N4-H40-N7	111.0
O4—H4…O2	2.473(3)	O4-H4-O2	166.0
O6—H6…O3	2.589(3)	O6-H6-O3	172.0
O9—H9…O8	2.677(2)	O9-H9-O8	174.0

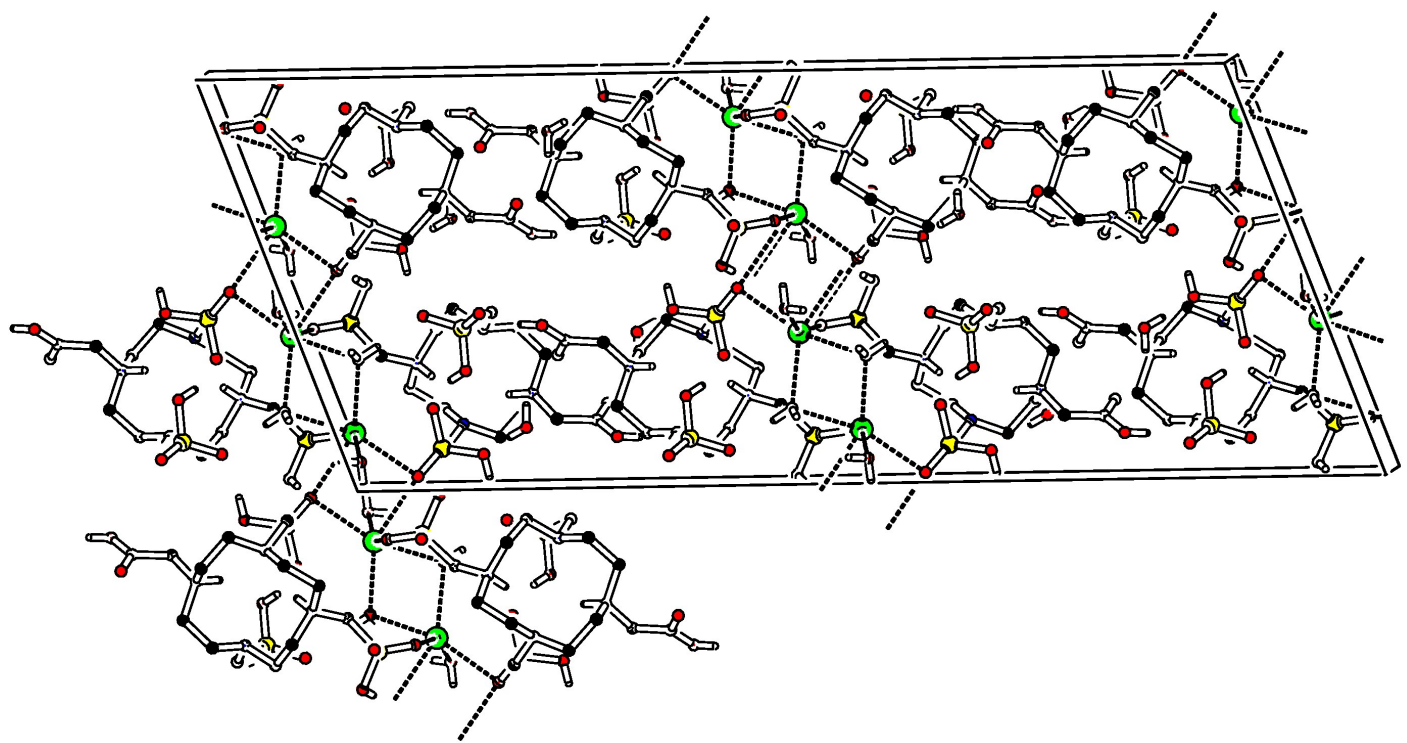


Figure S32: Crystal packing of $\text{KH}_6\text{doa}3\text{p}\cdot3\text{H}_2\text{O}$ in solid state. Atom labelling scheme: carbon (black), nitrogen (blue), oxygen (red), phosphorus (yellow), potassium (green). Bonds to K^+ cation are shown as dashed lines.

References:

1. J. M. Weeks, M. R. Tailor and K. P. Wainwright, *Dalton Trans.*, **1997**, 317–322.
2. G. Anderegg, F. Arnaud-Neu, R. Delgado, J. Felcman, K. Popov, *Pure Appl. Chem.*, 2005, **77**, 1445–1495.
3. S. Chaves, R. Delgado, J. J. R. Fraústo da Silva. *Talanta* 1992, **39**, 249–254.
4. P. Táborský, P. Lubal, J. Havel, J. Kotek, P. Hermann, I. Lukeš: *Collect. Czech. Chem. Commun.* 2005, **70**, 1909–1942.
5. M. P. C. Campello, S. Lacerda, I. C. Santos, G. A. Pereira, C. F. G. C. Geraldes, J. Kotek, P. Hermann, J. Vaněk, P. Lubal, V. Kubíček, É. Tóth, I. Santos, *Chem. Eur. J.* 2010, **16**, 8446–8465.
6. F. K. Kálmán, Z. Baranyai, I. Tóth, I. Bánya, R. Király, E. Brücher, S. Aime, X. Sun, A. D. Sherry, Z. Kovács, *Inorg. Chem.* 2008, **47**, 3851–3862.
7. M. P. C. Campello, M. Balbina, I. Santos, P. Lubal, R. Ševčíková, R. Ševčík, *Helv. Chim. Acta*, 2009, **92**, 2398–2413.
8. F. Kálmán, *PhD Thesis*, University of Debrecen, Hungary, **2007**.
9. (a) R. Delgado, L. C. Siegfried, T. A. Kaden. *Helv. Chim. Acta* 1990, **73**, 140–148; (b) R. Delgado, J. Costa, K. P. Guerra and L. M. P. Lima, *Pure Appl. Chem.*, 2005, **77**, 569–579.
10. Kabachnik I. M., Medved T. Ya., Belskii, F. I., Pisareva S. A.: *Izv. Akad. Nauk SSSR, Ser. Khim.* **1984**, 844–849.
11. T. Ya. Medved, M. Kabachnik, Belskii, F. I., Pisareva S. A. *Izv. Akad. Nauk SSSR, Ser. Khim.* **1988**, 2103–2107.
12. X. Sun, M. Wuest, Z. Kovacs, A.D. Sherry, R. Motekaitis, Z. Wang, A.E. Martell, M.J. Welch, C.J. Anderson, *J. Biol. Inorg. Chem.* 2003, **8**, 217–225.
13. a) P. Táborský, P. Lubal, J. Havel, J. Kotek, P. Hermann, I. Lukeš, *Collect. Czech. Chem. Commun.* 2005, **70**, 1909–1942; b) M. Försterová, I. Svobodová, P. Lubal, P. Táborský, J. Kotek, P. Hermann, I. Lukeš, *Dalton Trans.* **2007**, 535–549.
14. (a) M. Kývala, I. Lukeš, *International Conference on Chemometrics '95*, Pardubice, Czech Republic, 1995, p. 63; full version of “*OPIUM*” is available (free of charge) on <http://www.natur.cuni.cz/~kyvala/opium.html>; (b) M. Kývala, P. Lubal, I. Lukeš, *IX. Spanish-Italian, and Mediterranean Congress on Thermodynamics of Metal Complexes (SIMEC 98)*, Girona, Spain, 1998.
15. (a) A. E. Martell and R.M. Smith, *Critical Stability Constants*, Plenum Press, New York, 1974–1989, vol. 1–6; (b) A. E. Martell, R. M. Smith and R. J. Motekaitis, *NIST Standard Reference Database 46 (Critically Selected Stability Constants of Metal Complexes)*, Version 7.0, NIST Standard Reference Data, Gaithersburg, MD, 2003.
16. C. F. Baes, Jr. and R. E. Mesmer, *The Hydrolysis of Cations*, Wiley, New York, 1976.
17. I. Voráčová, J. Vaněk, J. Pasulka, Z. Střelcová, P. Lubal, P. Hermann, *Polyhedron* 2013, **61**, 99–104.
18. G. M. Sheldrik, *SHELXL97. Program for Crystal Structure Refinement from Diffraction Data*; University of Göttingen: Göttingen, Germany, 1997.